JASs Journal of Anthropological Sciences Open Access
Research articles Vol. 104 (2026), pp. 1 - 20 doi. 10.4436/jass.10404

Two methods of intentional cranial modification from Early Holocene Songhuajiang in Northeast China

Qiyu Yin[1,2], Qiang Li[1,2], Christopher J. Bae[3] & Xijun Ni[1,2,4]

1) Institute of Vertebrate Paleontology and Paleoanthropology, Chinese Academy of Sciences, 142 Xi Zhi Men Wai Street, Beijing, 100044, China
e-mail: nixijun@ivpp.ac.cn

2) University of Chinese Academy of Sciences, Beijing, 100049, China

3) Department of Anthropology, University of Hawai'i at Manoa, Honolulu, HI, USA
e-mail: cjbae@hawaii.edu

4) PaleoAnthropological Research Center, Fudan University, Shanghai, 200433, China

Summary - *Since its appearance at the terminal Pleistocene, intentional cranial modification ("ICM") and its implications have generated considerable scientific debate regarding how or why such a tradition arose. Here, we report on newly discovered human ICM crania from the Songhuajiang area in Northeast China, dating to the Pleistocene–Holocene transition. The materials include three partially damaged cranial specimens - PA1688 (11,641 – 11,270 cal BP), TPA2401 (11,825 – 11,601 cal BP) and TPA2402 (11,245 – 11,179 cal BP). Geometric morphometric analyses effectively distinguished modified and unmodified individuals, in addition to partially identifying variation in different modification types. PA1688 presents a typical tabular type, while TPA2401 and TPA2402 display traits of the annular type, a type not previously reported in this region. During the Early Holocene two types of ICM coexisted in the Songhuajiang region; a tradition that persisted for nearly 1,000 years. Further, there was no significant difference in the strontium isotope ratios between individuals with the different ICM. These results are consistent with two different ICM methods being practiced by local individuals in the Harbin region during the terminal Pleistocene–Holocene period, with no evidence linking either type to individuals of non-local origin.*

Keywords - *Intentional cranial modification, Geometric morphometrics, Stable isotope analysis.*

Introduction

Intentional Cranial Modification ("ICM") practices change the shape and thickness of the skull through various deforming devices (Khonsari et al. 2013). ICM practices first appears during the Terminal Pleistocene. A recently reported specimen from Arene Candide Cave, Italy (ca. 12,620–12,190 cal BP), may represent the earliest currently known example of ICM in Europe, expanding the geographic and temporal scope of the early evidence (Mori et al. 2025). Early evidence includes Nacurrie 1 (calibrated AMS ^{14}C date: 13,569–12,926 cal BP), Kow Swamp 5, and Coobool Creek 65 (no direct dates available; but contextual evidence suggests a terminal Pleistocene–early Holocene age) from the central Murray River region in southeastern Australia (Brown 2010; Langley et al. 2019). Additional early cases have been identified in the Middle East, including Shanidar cave, Iraq (ca. 11,000 to 10,500 BP), Ganj Dareh Tepe and Tepe Ghenil in Iran (ca. 9,500 to 8,500 BP and late 10th to early 8th millennium BP, respectively), and Bouqras, Syria (ca. 8,500 to 7,500 BP) (Soleki et al. 1992, 2004). The practice is documented in different regions of the world until the 20th century (Dingwall 1931).

Evidence from various sites and periods suggests that ICM has a long history in China, with diverse head-deforming methods emerging over time. The earliest evidence comes from

Northeast China. Early Neolithic individuals include PA1683 (11,245–11,200 cal BP) and PA1616 (11,095–10,745 cal BP) from Harbin with the tabular type, the Djalainor II cranium (AN624) from Djalainor, and Qianguo Man (approximately 10,000 and 7,800 BP, respectively; lacking precise radiocarbon dates) from Qingshantou, Jilin, both exhibiting the annular type (Ni et al. 2020; Suzuki 1950; Zhang and You 1985). During the Middle and Late Neolithic periods (around 7,000–4,000 BP), examples of ICM practice were most commonly found in North and Northwest China (Xiao 2014; Zhang and You 1985; Zhao et al. 2017). In the Xinjiang Uygur Autonomous Region, the most common ICM type is the annular type, characterized by posterosuperior elongation of the cranium and a sloping of the frontal and occipital bones (Zhang 2010). The deformed crania discovered in Dawenkou from Shandong Province around 5,500-4,300 BP featured slight flattening of the occipital bone, which is thought to be an unintended result of infants sleeping on a hard cradleboard (Pang 1993; Zhao et al. 2017). An ICM case from the Xishan site in Henan Province (6,000-5,000 BP) shows a post-occipital saddle-like depression and an oblique occipital bone, suggesting the use of a head-modification device (Pechenkina et al. 2009).

Given this geographic and temporal variability, researchers have sought more refined methods to study the nature of ICM. Earlier studies primarily focused on describing the typical features and using traditional morphometric techniques to classify modification types (Brown 2010; O'Brien and Stanley 2013). In recent years, with the development of 3D reconstruction techniques, geometric morphometrics has been attempted to better understand how ICM practice may influence craniofacial morphology (Ferros et al. 2014; Ross and Ubelaker 2009), the causes of inheriting ICM customs among different populations (Mayall and Pilbrow 2019; Perez 2007), and the distinction between different methods of cranial modification (Kuzminsky et al. 2016). These studies typically focus on well-preserved specimens with intact cranial landmarks suitable for geometric morphometric analysis. For damaged specimens or those exhibiting severe postmortem deformation, they often lack sufficient morphological features for reliable metric evaluation (Ricci et al. 2008). Under such limitations, landmark-based 3D geometric morphometric techniques may provide new insights for virtual reconstruction of damaged or distorted specimens, enabling them for further morphological comparisons.

These new techniques not only improved the analysis of damaged specimens, but also brought new possibilities for investigating their cultural and social significance. Although the Songhuajiang specimens are only partially preserved, they retain key morphological features that allow for the reconstruction and identification of ICM characteristics using geometric morphometrics (Gunz et al. 2009).

ICM practices in Northeast Asia appeared long before the appearance of sedentary lifeways and has been suggested to reflect aspects of social differentiation or status (Ni et al. 2020; Zhang et al. 2019). In other parts of the world, ICM has also been considered as a symbol of cultural identity or a means to distinguish different social groups (Tiesler 2013; Torres-Rouff and Yablonsky 2005). If different forms of cranial modification reflect culturally distinct groups, their presence within the same region could also be related to processes of migration or interaction between populations. It is essential to consider other contemporaneous ICM cases from broader Northeast China during the same period to investigate the transmission of ICM practices. In particular, the Djalainor II specimen (AN624) from Djalainor, on the western edge of the Hulunbuir region, Inner Mongolia Autonomous Region, provides an important comparative reference (Endo 1945). As the specimen has not been examined in sufficient detail regarding its modification, no firm conclusion has been reached about its specific type. Geographically, the Djalainor, Qingshantou, and Songhuajiang sites all located in Northeast China region and have comparable climatic and environmental conditions, as shown in Figure 1 (Suzuki 1950;

Zhang et al. 2019; Zhang and You 1985). These ICM cases may reflect possible interactions among these neighboring regions, and chronological evidence suggests a long-standing presence of ICM practices in Northeast China, offering a temporal reference point for comparisons with other ICM cases in East Asia. Therefore, in various ICM studies, strontium isotope ratios were used to identify presence of non-local individuals within ICM samples, revealing whether such cultural practices were associated with population movement (Knudson et al. 2004). For example, preliminary strontium isotope analyses of ICM individuals from Bavarian sites predominantly reflect local signatures, contradicting the hypothesis of late immigration (Schweissing and Grupe 2000).

To further explore these cultural interpretations, we conducted strontium isotope analysis on all intentionally modified crania from Songhuajiang to assess whether distinct groups were present (Bentley 2006). Strontium isotope analysis requires only minimal sample quantities and can be performed non-destructively using laser ablation, enabling investigations of individual origins, social identity, mobility, and cultural behavior (Bentley 2006; Copeland et al. 2011). Given the limited preservation of morphology necessary for traditional linear measurements, and the restricted amount of available bone, the combined application of geometric morphometrics and isotope analysis provides a powerful tool for interpreting the biological and cultural dimensions of the Songhuajiang ICM individuals while maximizing the information obtainable from these fragmentary remains.

Materials and methods

Materials

The three ICM specimens, PA1688 (11,641–11,270 cal BP), TPA2401 (11,825–11,601 cal BP) and TPA2402 (11,245–11,179 cal BP) were found in 2023 and 2024 in an underwater sand mine near Dadingzi Hill in the Songhuajiang River near Harbin City, Heilongjiang Province, China (Fig. 1). The specimens were located in the sedimentary layer of the Guxiangtun Formation. Two other ICM crania (PA1683, dated to 11,245–11,200 cal BP, and PA1616, dated to 11,095–10,745 cal BP) were unearthed from the same area previously and represent one of the earliest records of ICM practice in China (Ni et al. 2020). The newly found tabular modified cranium specimen PA1688 preserves only the parietal bones. There is damage to the meso-anterior margin of the left parietal bone, with the frontal angle missing (see Figure 3a). Only the frontal bone and the left parietal bone are preserved for TPA2401, with notable damage at the junction between the right frontal bone and the sphenoid bone (see Figure 3b). TPA2402 preserves both the frontal and parietal bones, although the right side is severely damaged (see Figure 3c).

***Fig. 1** - Map of northeast China. The asterisk indicates the fossil site.*

Therefore, in addition to the three newly discovered intentionally modified crania from the Songhuajiang area, several comparative specimens were included in our analysis: PA1683 and PA1616 with tabular modification, also from the Songhuajiang region; the Djalainor II specimen (AN624) from Djalainor; three annularly modified crania (models) from Peru; and four additional specimens with ICM features, all curated at the Institute of Vertebrate Paleontology and Paleoanthropology (IVPP), Beijing, China. The IVPP specimens exhibit annular type and

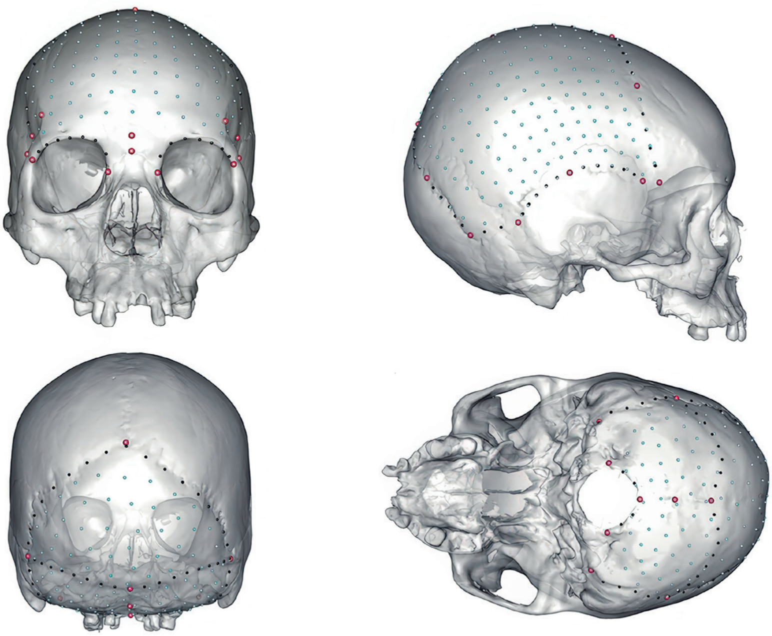

***Fig. 2** - Landmark Settings for GM (Geometric Morphometric) analysis. Red dots indicate fixed landmarks, black dots indicate landmarks on curves, and blue dots indicate landmarks on surfaces. The cranium is IVPP CO128. Top left: anterior view; top right: lateral view (right); bottom left: posterior view; bottom right: inferior view.*

another modification pattern likely produced using a hard, plate-like tool or a portable cradleboard—sometimes involving an anterior, oblique board that applies pressure to the occipital bone (Schijman 2005). This type of modification is often regarded as unintentional (Clark et al. 2007; Neumann 1942) and is hereafter referred to as Type III modification. For comparative unmodified specimens, we selected relatively well-preserved samples from the IVPP modern human collection. Most of these crania originate from North China and Yunnan Province (Southwest China), some originate from Europe. The detailed information of the comparative cranial materials is provided in Table S1.

3D Virtual Reconstruction

All archaeological and modern human specimens were scanned using Artec Space Spider high-resolution 3D surface scanner with a resolution of 0.1 mm. The scanner is housed in the Key Laboratory of Vertebrate Evolution and Human Origin, Chinese Academy of Sciences. Reconstruction of 3D surface data were performed in Artec Studio 17.

We performed the virtual reconstruction using the *mirror* function using the Autodesk Meshmixer software (Autodesk Inc.) version 3.5.474. The purpose of mirroring is the reflection of the non-defective side of the cranium onto the defective one to reconstruct the missing surface (Buonamici et al. 2018). For PA1688, we used bregma, lambda as the midline landmarks and the sagittal suture as the mid-sagittal axis, the preserved parietal eminences, squamous sutures, lambdoid sutures and most portions of the coronal suture were preserved, which provided adequate bilateral reference points for the reconstruction. For TPA2401 and TPA2402, we used nasion, glabella, bregma, and lambda as midline landmarks and the sagittal suture as the mid-sagittal axis. The bilateral reference structures for TPA2401 are dacryon, *frontomalare orbitale*, *frontomalare temporale*, superciliary arch, frontal eminence, and temporal line; for TPA2402, they are dacryon, superciliary arch, frontal eminence, and most portions of temporal lines. Then we used VG Studio 3.4 to get a clearer picture of the three new specimens, and we used different colors for the original and reconstructed parts of the specimens (see Figure 3).

Geometric morphometric analysis

The aim of GM analysis is to provide an independent, quantitative test of whether the morphological features of these highly fragmentary specimens support the conclusions based on our qualitative observations. Because the specimens are incompletely preserved, traditional morphological assessment alone may be insufficient for confident classification. GM analysis allows us to reconstruct the missing portions and evaluate the degree of morphological separation between modification types and helps interpret specimens with mixed or ambiguous features (e.g. specimen AN624) and addresses a broader methodological question: whether the visualization of GM-derived shape variation can detect the subtle modification-related shape signals in fragmentary cranial remains.

The landmark and semi landmark coordinates were generated in Stratovan Checkpoint software, comprising 31 landmarks, 13 curves consisting of 160 semi landmarks, and 3 patches consisting of 385 semilandmarks. The detailed landmark and semi landmark settings and positions are shown in Table S2, S3, S4 and Figure 2. GM analysis was performed in R 4.4.3 (R Core Team 2025). For the missing landmark reconstruction of frontal bones for TPA2401 and TPA2402 in the subsequent GM analysis, we used 'estimate. missing' function from the *geomorph* package (method = "TPS"). For TPA2401, we used the preserved left parietal bone, as the right side was not available. Since all parietal landmarks in our dataset were defined on the left side, we mirrored the landmarks accordingly. Curve and surface semi landmarks were slid to minimize bending energy and all landmarks were aligned using

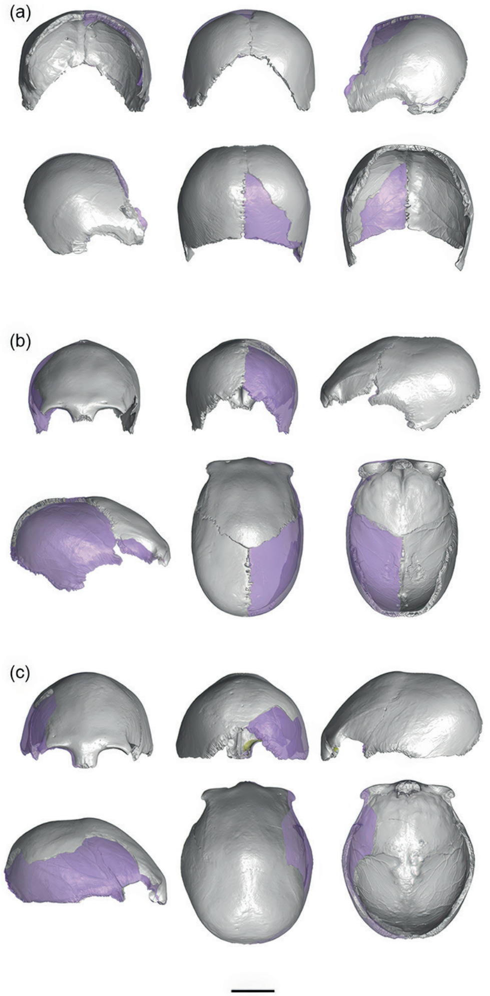

***Fig. 3** - Visual reconstruction of specimen PA1688 (a), TPA2401 (b), and TPA2402 (c). The purple areas represent the visualized results of the virtual symmetry restoration, which were mirrored from the counterpart. Scale bar = 5cm. Top left to right: anterior view, posterior view, left view; bottom left to right: right view, top view, bottom view.*

Generalized Procrustes Analysis (GPA) using the 'gpagen' function in the *geomorph* package (Adams et al. 2016). GPA aims to eliminate any influences of translation, scaling, and rotation factors. We used between-group PCA (Principal Component Analysis) to analyze the specimens to compare shape variations across different cranial regions and identify ICM patterns specific to different regions. The PCA were performed using the *gm.prcomp* function in the *geomorph* package (Adams et al. 2016). For the visualization of localized morphological variation, we used the 'findMeanSpec' function to identify the specimen most representative of the unmodified group's mean shape, and the 'localmeshdiff' function from the *Arothron* package to measure the extent of local shape deviations between target and reference specimens (Profico et al. 2021).

Radiocarbon dating and strontium isotope analysis

All five specimens are currently curated in the Institute of Vertebrate Paleontology and Paleoanthropology (IVPP). Three new specimens (PA1688, TPA2401 and TPA2402) were radiocarbon dated. Cortical bones were taken from the left parietal bone near the sagittal suture in PA1688, from the frontal bone near the right temporal line in TPA2401, and from the left parietal bone near the mastoid angle in TPA2402. Three samples of ICM crania were sent to BETA Laboratories (Miami, Florida, USA) for radiocarbon dating. Pretreatment was conducted at the Beta Analytic using standard acid-base-acid (ABA) procedures, and collagen was extracted prior to AMS measurement. The results were certified by ISO/IEC-17025:2005. Radiocarbon dates were calibrated using OxCal v4.4 and the IntCal20 calibration curve.

For the strontium isotope analysis, we followed the procedure described in Wang et al. (2016). Approximately 10 mg of cortical bone was sampled from each of the Songhuajiang specimens (PA1616, PA1683, PA1688, TPA2401, TPA2402), and ultrasonically cleaned with deionized water before ashing at 750°C for 8 hours. Samples were then dissolved in HCl, evaporated, redissolved in HNO_3, and purified using Sr-selective resin columns. Strontium isotope ratios were analyzed on a Finnigan MAT262 TIMS at the Institute of Geology and Geophysics, Chinese Academy of Sciences. All $^{87}Sr/^{86}Sr$ ratios were normalized to the NBS-987 standard (0.71025).

Results

Description of the newly found ICM crania

PA1688 preserves only left and right parietal bones. There is damage to the anterior part of the left parietal bone near the sagittal suture (see Figure 3a). The sagittal suture shows no clear evidence of closure, the coronal and lambdoid suture are nearly unfused, suggesting that the individual was relatively young. Bilateral parietal nodules protrude laterally, particularly on the right side, resulting in extreme maximum parietal breadths (Anton 1989). The sagittal sinus is partially preserved and appears as a shallow groove, with no signs of compression or flattening caused by external forces. Two prominent primary branches of the middle meningeal arteries are visible on each side. The anterior branch is thicker and deeper, with more terminal branches compared to the posterior branch, different from the typical pattern observed in unmodified crania, where both branches are similar in size and shape (Dean 1995).

Both TPA2401 and TPA2402 have high, flattened frontal bones, although the right side of both of their frontal bones is damaged (Fig. 3b,c). Partial parietal bones are also preserved. In TPA2401, the left parietal bone is well-preserved, while the right is completely absent. In contrast, TPA2402 retains relatively intact parietal bones, although the mastoid angles are missing bilaterally. The coronal and mid-sagittal sutures in TPA2402 show a higher degree of fusion compared to TPA2401, suggesting that TPA2402 represents an older individual. Both specimens exhibit blunt supraorbital margins, prominent temporal lines, and modest superciliary arches. Frontal eminences are more clearly observed bilaterally in TPA2401. The parietal bone of TPA2401 displays a more pronounced central elevation, whereas that of TPA2402 appears relatively flat. Regarding endocast morphology, TPA2402 has more developed terminal branches of the middle meningeal vessels compared to TPA2401. Additionally, multiple wormian bones are present along the left side of the sagittal suture in TPA2401—a trait frequently associated with ICM (O'Loughlin 2004).

Tab. 1 - Craniometric measurements of all studied and comparative specimens (mean values were calculated using data from Yin et al. 2022).

SPECIMEN NAME	TYPE	FRONTAL CHORD (MM)	FRONTAL SUB HEIGHT (MM)	FRONTAL CURVATURE INDEX (MM)	PARIETAL CHORD (MM)	PARIETAL SUB HEIGHT (MM)	PARIETAL CURVATURE INDEX (MM)
PA1688	unclassified specimen	-	-	-	112.01	32.29	28.83
TPA2401	unclassified specimen	122.03	20.68	16.95	99.71	25.17	25.24
TPA2402	unclassified specimen	138.03	24.92	18.05	102.74	21.93	21.35
AN624	unclassified specimen	125.24	15.01	11.98	110.47	30.86	27.94
AN2375	type III	108.13	21.08	19.50	103.47	30.23	29.22
CO314	annular	117.45	17.57	14.96	110.30	28.61	25.94
CO316	type III	111.20	22.53	20.26	97.72	26.48	27.10
CO361	annular	118.61	14.54	12.26	110.38	25.59	23.18
CO365	annular	126.10	16.16	12.82	102.06	26.63	26.09
BC115	annular	114.59	16.11	14.06	95.80	24.71	25.79
BC200	annular	134.02	14.52	10.83	100.58	39.52	39.29
BC201	annular	126.82	12.52	9.87	97.02	37.66	38.82
PA1616	tabular	118.49	18.9	15.9	107.61	23.86	22.2
PA1683	tabular	126.07	17.78	14.1	96.28	26.61	27.6
mean (n=121)	undeformed	110.30	25.68	23.28	116.85	24.91	21.28

In the deforming process, the devices are commonly placed on the neurocranium, and thus the effects of ICM are most prominent in the calvaria. In unmodified human crania, the calvaria maintains a rounded, bilaterally symmetrical head shape with moderate curvature. In contrast, the three ICM crania (PA1688, TPA2401, TPA2402) display morphological traits exceeding the normal range of unmodified crania.

Both TPA2401 and TPA2402 exhibit a sloping forehead and pronounced anteroposterior elongation, resulting in a more cylindrical cranial shape (see Figure 3b and 3c), which aligns with the characteristic feature of annular deformation (Gerszten and Gerszten 1995; Khonsari et al. 2013). The frontal chord measurements for unmodified crania have an average of 110.30 mm (Yin et al. 2022), while those for TPA2401 and

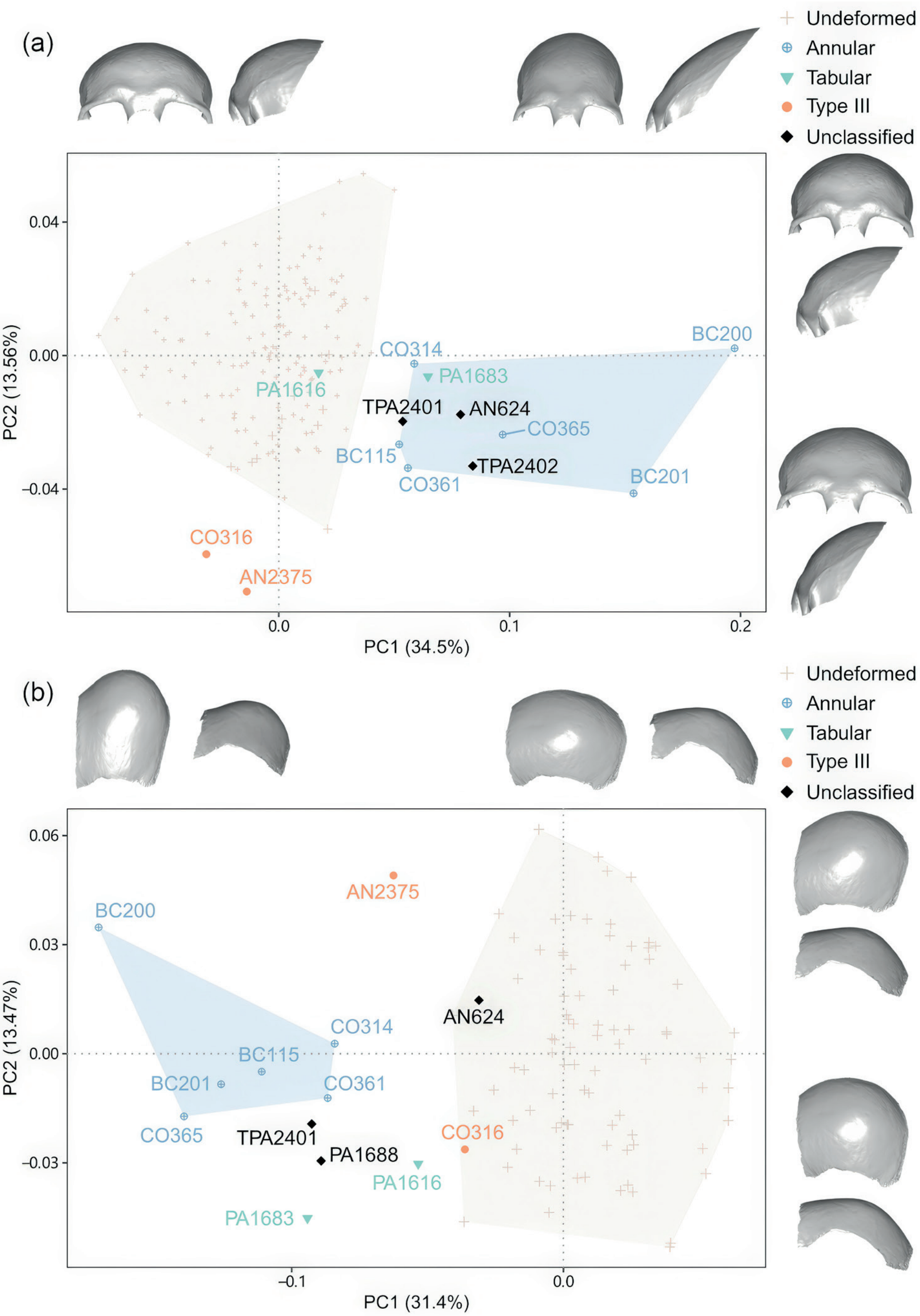

***Fig. 4(a,b)** - PCA (Principal Component Analysis) on the morphology of intentionally modified and unmodified human craniums. (a) frontal, (b) parietal. The images on the left and bottom are anterior and lateral views of the reconstructed extreme shapes of the first two PCs.*

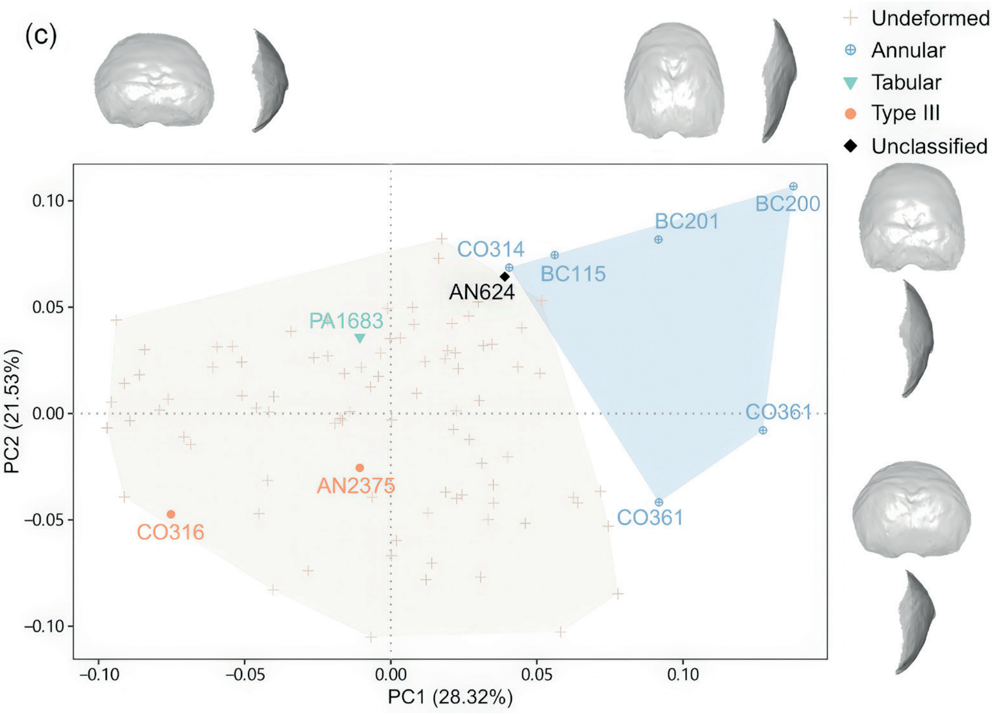

Fig. 4(c) ***- PCA (Principal Component Analysis) on the morphology of intentionally modified and unmodified human craniums. (c) occipital. The images on the left and bottom are anterior and lateral views of the reconstructed extreme shapes of the first two PCs.***

TPA2402 are 122.03 mm and 138.03 mm, far exceeding those observed in unmodified human crania. Moreover, the measurements for frontal curvature index for both specimens are significantly lower than the normal range, consistent with severe flattening resulting from the compressive forces. Another feature observed in the frontal bones is a significant thickening near the coronal margin anterior to the bregma, commonly found in specimens with annular type (Khonsari et al. 2013). Both TPA2401 and TPA2402 display depressions on the forehead caused by banding constraints, differing from the localized flattening seen in individuals with tabular type (e.g., PA1616 and PA1683), providing further evidence that TPA2401 and TPA2402 are different from the previously identified cases of tabular type.

The parietal curvature index (PCI) is another indicator of intentionally modified crania (Brown 2010). The PCI of PA1688 is 28.83, which falls outside the typical range of non-modified crania (14.10 to 28.07, with an average of 21.28). This value reflects lateral expansion of the parietal bones, likely caused by compression on the anterior and posterior regions of the cranium, with internal pressures redirected to the less restricted lateral areas (Püschel et al. 2020). The PCI values of TPA2401 (25.24) and TPA2402 (21.35) both fall within the non-modified range.

For comparative analysis, we included the Djalainor II skull (hereafter referred to as AN624) and specimens AN2375, CO314, CO316, CO361, CO365, BC115, BC200, and BC201, all of which display distinctive morphological features associated with ICM practices. Based on their linear measurements (see Table 1), all presumed ICM cases show a significantly

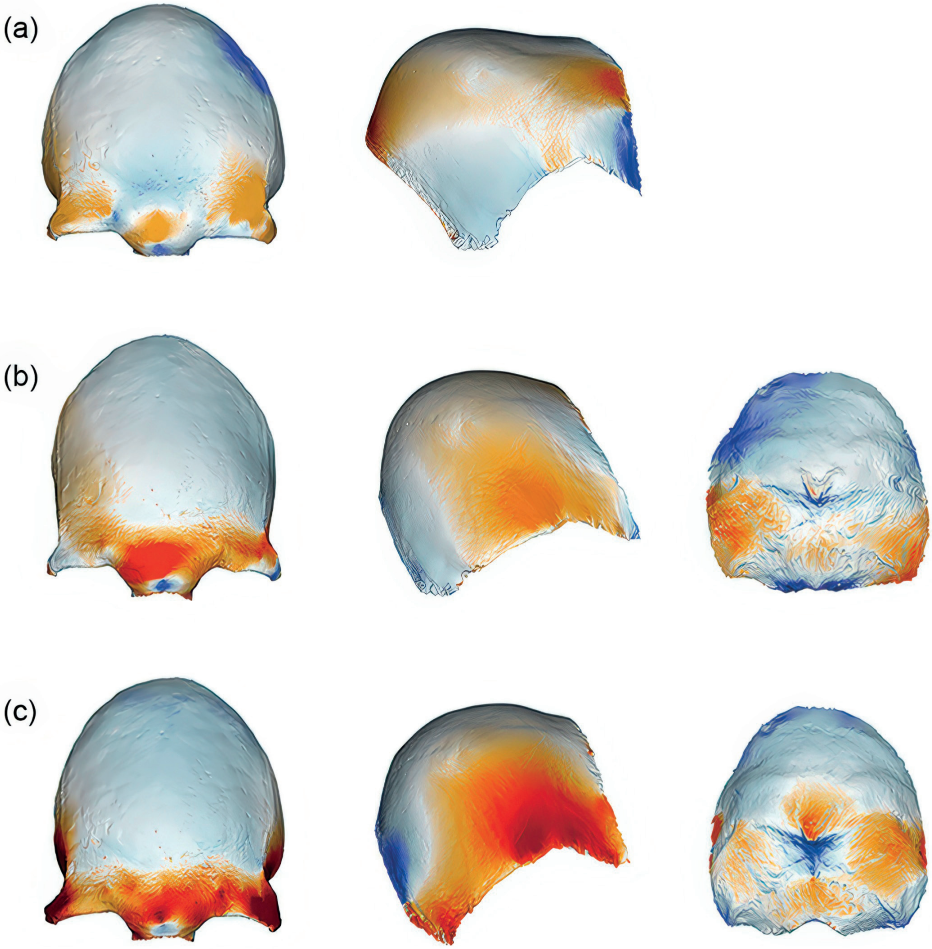

Fig. 5 - Visualization of regional variations across different ICM types. Frontal, parietal, occipital views are shown for three specimens: TPA2401 (a, annular), PA1683 (b, tabular) and AN624, each compared with the specimen most representative of the mean shape for unmodified group.

lower frontal curvature index, and a higher parietal curvature index compared to unmodified individuals. Specimens with more pronounced cranial modifications (e.g., BC200 and BC201) tend to exhibit greater deviations in these two indicators. These findings help us determine whether an individual was subjected to ICM practices and provides insight into the extent and variation in the severity of cranial modification.

Geometric morphometric analysis

The analysis of frontal bones reveals significant morphological differences in frontal shape between non-ICM and ICM crania. The first two principal components of PCA (accounting for 48.06% of the total variance) are presented in Figure 4a. The first principal component separates annularly modified crania from unmodified ones based on overall frontal shape, while the second principal component reflects the degree of frontal flatness, with higher PC2 scores corresponding to a more prominent forehead and a posteriorly positioned bregma. The frontal bone morphology of the two new specimens from the Songhuajiang area (TPA2401 and TPA2402 marked with black diamonds in Figure 4) belongs to the annular group, AN624 specimen is also positioned within this group.

We next examined the parietal bones; the results are shown in Figure 4b. The first two principal components accounted for 44.87% of the total variance. For the parietal analysis, specimens with lower PC1 scores represent an overall elongated shape with a strong protrusion towards the posterior-superior direction, which is consistent with annular modification. The PC2 score mainly reflects the degree of posterior cranial flattening, as stabilizing the back of the head with a board will result in significant flattening of the posterior parietal and occipital regions, therefore the tabular group has lower PC2 scores than the annular group. TPA2401 is closer to the annular group, PA1688 is closer to the tabular type in morpho space, while AN624 cannot yet be assigned to any ICM group.

For the occiput, among the specimens under evaluation, only AN624 has an intact occipital bone. PA1683 was symmetrically reconstructed for analysis. The results shown in Figure 4c indicate individuals with annular type have the highest scores on the PC1 axis, suggesting an overall elongated and flattened shape. PC2 mainly reflects the position of the occipital protuberance. The occipital shape of AN624 plots at the boundary between unmodified and annular groups, showing greater similarity with the unmodified group.

Overall, among the different cranial regions analyzed, the parietal bones provide the greatest ability to distinguish between modification types. In contrast, the frontal and occipital bones show limited ability, which may be due to factors such as sample size, preservation, or differences in how modification-related features are reflected in these regions.

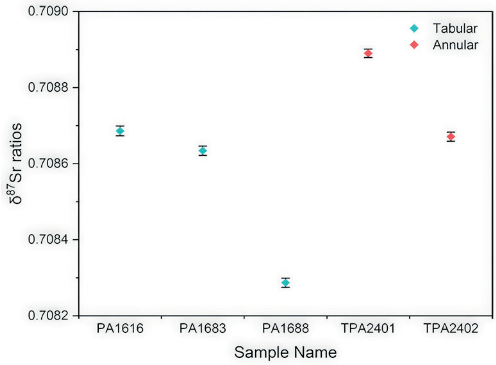

***Fig. 6** - Scatter plot of strontium isotope values for Songhuajiang individuals with 2σ error bars.*

To further assess the classification of the three specimens, we performed linear discriminant analyses (LDA) separately on the first 20 principal components (cumulative variance >90%) derived from the frontal, parietal, and occipital landmark configurations (see Table S5). However, due to the extremely small and highly unbalanced sample sizes in some groups, the LDA results should be interpreted with caution, as the group-specific parameters cannot be reliably estimated.

For comparison, the analyses using only the pre-reconstruction landmark configurations for the frontal and occipital regions are provided in the supplementary materials (Fig. S3 shows the landmark settings, and Fig S4 presents the results of these analyses).

Visualization of regional variations

We also visualized the morphological differences in the frontal, parietal, and occipital bones among the archaeological specimens (TPA2401, PA1683 and AN624) compared with the specimen most representative of the mean shape for unmodified group (Fig. 5). The specimens closest to the average morphology we selected as reference standards were: IVPP YNO93 for the frontal, IVPP OA66 for the parietal, and IVPP YNO146 for the occipital region). Red areas indicate expansion, and blue areas indicate contractions. As shown in Figure 5, both PA1683 and AN624 exhibit more pronounced expansion in the lower part of the

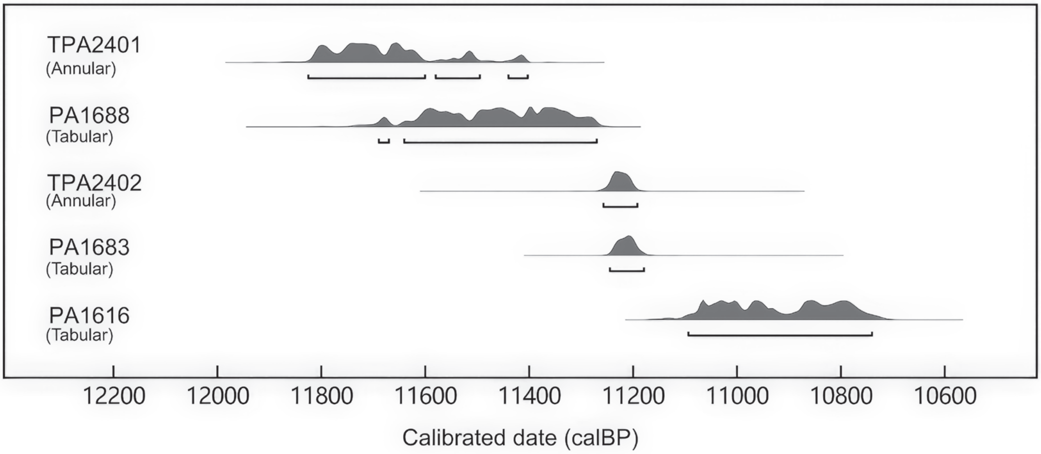

***Fig. 7** - The temporal overlap of calibrated radiocarbon dates for the two ICM types.*

frontal bone compared to TPA2401. In contrast, TPA2401 with annular type displays a notable contraction near the bregma. Regional variation in the parietal bone (Fig. 5a) shows that TPA2401 presents a depression near the squamous suture, likely caused by bandage wrapping, while the superior portion of the bone exhibits significant lateral expansion. In comparison, PA1683 with tabular type shows anterior and posterior contraction of the parietal bone. This pattern is consistent with the compressive forces applied by modification tools on the frontal and occipital bones, which redirected the growth of the parietal bone and caused the central area to expand outward (Püschel et al. 2020). Regarding the occipital bone, PA1683 shows expansion in the lower part and contraction in the upper region. This is likely due to the pressure applied via a board on the upper occipital region.

For AN624 (Fig. 5c), exhibits similar characteristics as PA1683, both showing anterior and posterior constriction with central expansion, which is a clear indication of compression on the frontal and occipital bones. Additionally, clear compression marks from a rigid tool are visible on the posterior side, while the lower occipital bone exhibits an expansion. These features align with the characteristics of tabular type or at least a unilateral compression by a rigid tool.

Preliminary isotope observations

The five ICM individuals show $\delta^{13}C$ values ranging from -19.9‰ to -22.9‰, and $\delta^{15}N$ values ranging from 11.4‰ to 12.9‰ (see Table 2 for results), indicating a diet dominated by C_3-based terrestrial resources with high animal protein intake, which is commonly associated with hunter-gatherer populations (DeNiro and Epstein 1978; Katzenberg 2008).

To test whether the individuals with different ICM methods originated from the same local population, we conducted strontium isotope analysis on all five ICM specimens from the Songhuajiang region. FTIR analyses are available for three of the five samples. The results shown in Table 3 and Figure 6 indicate that the strontium isotope ratios of all specimens fall within the range of the local strontium isotope values near the Harbin area in the Songhuajiang region (0.7080-0.7100) (Wang and Tang 2020). No clear differences were observed between the strontium isotope ratios of the two ICM groups (Fig. S5). In other words, the individuals all likely originated from the same local population.

However, it should be revealed that the usage of human bones for strontium isotope analysis has potential limitations (Nelson et al. 1986). Because only the cranial vault fragments were available for

Tab. 2 - Calibrated radiocarbon dates and isotope results of Songhuajiang specimens.

SPECIMEN NAME	LABORATORY NUMBER	UNCALIBRATED RADIOCARBON AGE	CALIBRATED RADIOCARBON AGE	Δ^{13}C VALUE (IRMS)	Δ^{15}N VALUE (IRMS)
PA1616	Beta - 446746	9490 +/- 30 BP	11,095 – 10,745 BP	-19.9‰	12.6‰
PA1683	Beta - 446745	9740 +/- 30 BP	11,245 – 11,200 BP	-20.8‰	11.4‰
PA1688	Beta - 589532	9990 +/- 40 BP	11,641 – 11,270 BP	-21.9‰	11.8‰
TPA2401	Beta - 689297	10100 +/- 30 BP	11,825 – 11,601 BP	-22.3‰	12.9‰
TPA2402	Beta - 690862	9780 +/- 30 BP	11,245 – 11,179 BP	-22.9‰	12.6‰

Tab. 3 - Sr isotope results of Songhuajiang specimens.

SPECIMEN NAME	^{87}SR/^{86}SR (REPORTED)	2Σ	NIST SRM-987	2Σ OF THE STANDARD	CORRECTED ^{87}SR/^{86}SR
PA1616	0.708703	0.000012	0.710267	0.000012	0.708686
PA1683	0.708651	0.000013	0.710267	0.000013	0.708634
PA1688	0.708304	0.000012	0.710267	0.000012	0.708287
TPA2401	0.708911	0.000011	0. 710271	0.000012	0.708890
TPA2402	0.708692	0.000012	0.710271	0.000012	0.708671

analysis, strontium isotope ratios were obtained from bone rather than teeth. As bone is subject to diagenetic alteration after burial, it may cause the $^{87}Sr/^{86}Sr$ values to shift toward the local environmental strontium signature (Bentley 2006; Budd et al. 2000). To assess the preservation state of the bone mineral, FTIR-derived indicators were measured for three of the five individuals (see Table S6), and representative spectra are shown in Figure S6, indicating generally good preservation. Because of these constraints, the $^{87}Sr/^{86}Sr$ results presented here are interpreted cautiously and are treated as preliminary data and discussed in conjunction with our published analysis.

Discussion

In recent years, new fossil discoveries have pushed the history of ICM further back. In Northeast Asia, the earliest ICM evidence was previously dated to the early Holocene (Ni et al. 2020). The discovery of TPA2401 extended the timeline to 11,825 – 11,601 cal BP. TPA2401 is the earliest known ICM case identified in the Songhuajiang area to date, its maximum age actually crosses the Pleistocene-Holocene boundary and places the ICM age into the late Pleistocene Younger Dryas period. The youngest ICM specimen in Songhuajiang (PA1616) dates back to 11,095 – 10,745 cal BP, as reported. Together, these findings demonstrate that ICM was practiced in the Songhuajiang area for nearly a millennium during the Late Pleistocene and the Early Holocene. This suggests that intentional cranial modification was a long-standing and persistent cultural phenomenon.

Previous morphometric studies on ICM (Seguchi et al. 2023) have applied 3D visualization methods of cranial outer surfaces to relatively well-preserved crania from Early historic Japan. Our study also employs 3D geometric morphometric methods on highly fragmented Early Holocene specimens, highlighting the feasibility and advantages of this approach for ancient, highly fragmented materials.

Our geometric morphometric analysis identified PA1688 as closer to the tabular type, characterized by pressure applied to the frontal and occipital bones, similar to previously reported specimens PA1616 and PA1683. AN624 also shows pressure on the anterior and posterior neurocranium, which is consistent with tabular modification. In contrast, TPA2401 and TPA2402 from the same location and chronological range display annular type.

Notably, the temporal overlap of two distinct ICM types implies the coexistence of multiple methods used for this practice within the same region (Fig. 7). PA1688, like the previously reported individuals PA1683 and PA1616, most likely exhibits tabular cranial modification, while two other contemporaneous crania from Harbin (TPA2401 and TPA2402) display annular modification—a method not previously documented in this region. One possible explanation is that one of these groups originated externally, using ICM as a way to distinguish their identity from that of local populations, as observed in Tiwanaku society in high-altitude Bolivia (Blom 2005). Another explanation is that the presence of multiple ICM types within the same population are associated with cultural groups or historical phases, similar to patterns observed in the Eurasian steppes after the conquest of the Huns (Torres-Rouff and Yablonsky 2005). A third possibility is that ICM variation corresponds to social roles or hierarchy. Studies of pre-Columbian Peru suggest that males with occipital modification type might have held higher social ranks compared to those with fronto-lambdoid modification (Okumura 2014).

Strontium isotope analysis of the Songhuajiang specimens shows no evidence suggesting that they belong to distinct populations with different geological origins. Among the three previously proposed possibilities, the first can be preliminarily excluded, as the isotopic data indicate that the ICM individuals shared a similar geological background. During its persistence, the strontium isotopic homogeneity of ICM individuals in the region reflects a sustained cultural continuity through the early interval, placing Northeast China within the wider Pleistocene context of the practice. In this context, it is important to clarify that Djalainor II (AN624) specimen exhibits a tabular type, because in regional studies, the distribution of modification types allows us to observe the differences in their technical choices and shaping preferences. Across Northeast China, tabular modification techniques documented at multiple Early Holocene sites may reflect that this technique was widespread in the region and provide a basis for comparing technological practices across early sites.

However, on a broader scale, the geographic distribution of ICM has prompted discussion of possible interregional diffusion. ICM cases show a particularly high frequency in the Americas, making the Americas an important area to consider in discussions of possible role of population migration in introducing the practice (Cocilovo et al. 2011; Rhode 2001). Previous research has suggested that ICM in the Americas may have an Asiatic origin, potentially introduced by the First Americans as they migrated across Beringia (Narang et al. 2023; Schijman 2005).

This hypothesis is supported by various forms of indirect evidence. Cases of occipital flattening discovered in the northernmost Americas indicates possible early trans-Pacific contacts (Emmick 2001; Ossenberg 1977). Ancient DNA studies further reveal close genetic relationship between the ancient American populations and the ancient Siberian and ancient northern East Asians populations, supporting the potential influences of these practices through population movements (Sikora et al. 2019; Willerslev and Meltzer 2021; Zhang and Fu 2020). From the perspective of archaeological remains, the presence of microblade technology, as a key adaptation strategy for Late Pleistocene Northeast Asian populations in high-latitude environments, highlighted technological similarities between the Late Pleistocene Northeast Asia and the First Americans (Kuzmin et al. 2007; Norton et al. 2007; Waters 2019). Specifically, the preparation of wedge-shaped cores requires careful platform trimming and a systematic flaking sequence, which exhibits technological similarities across these regions (Chen and Wang 1989; Yi et al. 1985). Taken together, the convergence of geological, genetic, and technological evidence highlights the potential relevance and importance of Northeast Asian evidence for understanding the early distribution and possible transmission of this practice into the Americas.

Our study highlights the coexistence of two ICM types in the early Holocene of Northeast China and indicates that this practice existed in the region for at least nearly one thousand years. The presence of both annular and tabular ICM types in the terminal Pleistocene-Holocene Northeast China suggests that ICM custom was not only practiced earlier than previously known, but also have exhibited a degree of variation in modification form and technique. This morphological diversity suggests that ICM practices could have been adapted to individual preferences or adjustments in different social or functional contexts. The techniques used to create ICM allowed for a degree of flexibility, and was likely to carry some social significance, potentially showing the individual's social identity, gender or status. While the motivations and social meanings of these customs remain unclear, their early appearance and morphological differentiation point to a more complex pattern rather than a single, homogeneous tradition.

Data availability

The data measurements on modern human specimens used for comparisons are available at Yin et al. (2022), "A 10 ka intentionally deformed human skull from Northeast Asia", https://doi.org/10.1002/oa.3104, International Journal of Osteoarchaeology. Information regarding the human cranial specimens used in this study is available in Supplementary Table S1. The data that supports the geometric morphometric analysis results of this study are available from the corresponding author upon reasonable request.

Acknowledgements

This project has been supported by the National Key Research and Development Program of China (2023YFF0804502), the National Natural Science Foundation of China (42488201, 41988101). We would like to thank Yemao Hou and Ning Ma for their technical support, and Dan Lu and Yinan Zhang for insightful discussions on analytical methods. Finally, we would like to acknowledge the China Scholarship Council (CSC), as well as the University of Hawai'i at Manoa, particularly the Department of Anthropology, College of Social Sciences for providing financial and academic support of this research.

Author contributions

Qiyu Yin - *data curation (lead), formal analysis (lead), investigation (equal), methodology (equal), software (lead), writing – original draft (lead), writing – review and editing (supporting).*
Qiang Li - *conceptualization (supporting), formal analysis (supporting), investigation (equal), project administration (supporting), supervision (equal), writing – review and editing (supporting).*
Christopher J. Bae - *conceptualization (equal), formal analysis (supporting), methodology (equal), investigation (supporting), project administration (lead), supervision (equal), writing – review and editing (lead).*

Xijun Ni - *conceptualization (lead), data curation (supporting), formal analysis (supporting), investigation (equal), methodology (equal), project administration (lead), funding acquisition (lead), supervision (equal), software (supporting), writing – review and editing (equal).*

References

Adams DC, Collyer M, Kaliontzopoulou A, et al (2016) Geomorph: Software for geometric morphometric analyses.

Anton SC (1989) Intentional cranial vault deformation and induced changes of the cranial base and face. Am J Phys Anthropol 79: 253-267. https://doi.org/10.1002/ajpa.1330790213

Bentley RA (2006) Strontium isotopes from the earth to the archaeological skeleton: a review. J Archaeol Method Theory 13: 135-187. https://doi.org/10.1007/s10816-006-9009-x

Blom DE (2005) Embodying borders: human body modification and diversity in Tiwanaku society. J Anthrop Archaeol 24: 1-24. https://doi.org/10.1016/j.jaa.2004.10.001

Brown P (2010) Nacurrie 1: Mark of ancient Java, or a caring mother's hands, in terminal Pleistocene Australia? J Hum Evol 59: 168-187. https://doi.org/10.1016/j.jhevol.2010.05.007

Budd P, Montgomery J, Barreiro B, et al (2000) Differential diagenesis of strontium in archaeological human dental tissues. Appl Geochem 15: 687-694. https://doi.org/10.1016/S0883-2927(99)00069-4

Buonamici F, Furferi R, Genitori L, et al (2018) Reverse engineering techniques for virtual reconstruction of defective skulls: an overview of existing approaches. Comput Aided Des Appl 16: 103-112. https://doi.org/10.14733/cadaps.2019.103-112

Chen C, Wang X-Q (1989) Upper Paleolithic microblade industries in North China and their relationships with Northeast Asia and North America. Arct Anthropol 26: 127-156.

Clark JL, Dobson SD, Antón SC, et al (2007) Identifying artificially deformed crania. Int J Osteoarchaeol 17: 596-607. https://doi.org/10.1002/oa.910

Cocilovo JA, Varela HH, O'Brien TG (2011) Effects of artificial deformation on cranial morphogenesis in the South Central Andes. Int J Osteoarchaeol 21: 300-312. https://doi.org/10.1002/oa.1141

Copeland SR, Sponheimer M, de Ruiter DJ, et al (2011) Strontium isotope evidence for landscape use by early hominins. Nature 474: 76-78. https://doi.org/10.1038/nature10149

Dean VL (1995) Sinus and meningeal vessel pattern changes induced by artificial cranial deformation: A pilot study. Int J Osteoarchaeol 5: 1-14. https://doi.org/10.1002/oa.1390050102

DeNiro MJ, Epstein S (1978) Influence of diet on the distribution of carbon isotopes in animals. Geochim Cosmochim Acta 42: 495-506. https://doi.org/10.1016/0016-7037(78)90199-0

Dingwall EJ (1931) Artificial cranial deformation: a contribution to the study of ethnic mutilations, Bale.

Emmick J (2001) Effects of Koniag artificial cranial deformation on Eskimo population comparisons. (Master's), The University of Montana.

Endo R (1945) On the Djalainor skulls. Proceedings of the Japan Academy 21: 435-443. 1 https://doi.org/0.2183/pjab1945.21.435

Ferros I, Mora MJ, Obeso IF, et al (2014) The nasomaxillary complex and the cranial base in artificial cranial deformation: relationships from a geometric morphometric study. Eur J Orthod 37: 403-411. https://doi.org/10.1093/ejo/cju066

Gerszten PC, Gerszten E (1995) Intentional cranial deformation: a disappearing form of self-mutilation. Neurosurgery 37: 374-382.

Gunz P, Mitteroecker P, Neubauer S, et al (2009) Principles for the virtual reconstruction of hominin crania. J Hum Evol 57: 48-62. https://doi.org/10.1016/j.jhevol.2009.04.004

Katzenberg MA (2008) Stable isotope analysis: a tool for studying past diet, demography, and life history. In: Katzenberg MA, Grauer AL, Biological anthropology of the human skeleton, Wiley Blackwell, p. 467-504.

Khonsari R, Friess M, Nysjö J, et al (2013) Shape and volume of craniofacial cavities in intentional skull deformations. Am J Phys Anthropol 151. https://doi.org/10.1002/ajpa.22263

Knudson KJ, Price TD, Buikstra JE, et al (2004) The use of strontium isotope analysis to investigate Tiwanaku migration and mortuary ritual in Bolivia and Peru. Archaeometry 46: 5-18. https://doi.org/10.1111/j.1475-4754.2004.00140.x
Kuzmin Y, Keates S, Shen C (2007) Origin and spread of microblade technology in Northern Asia and North America, Archaeology Press, Burnaby, Canada.
Kuzminsky SC, Tung TA, Hubbe M, et al (2016) The application of 3D geometric morphometrics and laser surface scanning to investigate the standardization of cranial vault modification in the Andes. Archaeol Sci Rep 10: 507-513. https://doi.org/10.1016/j.jasrep.2016.11.007
Langley MC, Clarkson C, Ulm S (2019) Symbolic expression in Pleistocene Sahul, Sunda, and Wallacea. Quat Sci Rev 221: 105883. https://doi.org/10.1016/j.quascirev.2019.105883
Mayall P, Pilbrow V (2019) A review of the practice of intentional cranial modification in Eurasia during the migration period (4th – 7th c AD). J Archaeol Sci 105: 19-30. https://doi.org/10.1016/j.jas.2018.12.007
Mori T, Sparacello VS, Riga A, et al (2025) Early European evidence of artificial cranial modification from the Italian Late Upper Palaeolithic Arene Candide Cave. Scientific Reports 15: 27792. https://doi.org/10.1038/s41598-025-13561-8
Narang P, Jandial Z, Aramayo JDB, et al (2023) Artificial cranial deformation in Tiwanaku, Bolivia. Child's Nervous System 39: 3051-3055. https://doi.org/10.1007/s00381-023-06094-w
Nelson BK, Deniro MJ, Schoeninger MJ, et al (1986) Effects of diagenesis on strontium, carbon, nitrogen and oxygen concentration and isotopic composition of bone. Geochim Cosmochim Acta 50: 1941-1949. https://doi.org/10.1016/0016-7037(86)90250-4
Neumann GK (1942) Types of artificial cranial deformation in the Eastern United States. Am Antiq 7: 306-310. https://doi.org/10.2307/275486
Ni X, Li Q, Stidham TA, et al (2020) Earliest-known intentionally deformed human cranium from Asia. Archaeol Anthropol Sci 12: 93. https://doi.org/10.1007/s12520-020-01045-x
Norton CJ, Bae K, Lee H, et al (2007) A review of Korean microlithic industries. In: Kuzmin Y, Keates S, Shen C, Origin and spread of microblade technology in Northern Asia and North America, Simon Fraser University Press, Burnaby, B.C., p. 91-102.
O'Brien TG, Stanley AM (2013) Boards and cords: discriminating types of artificial cranial deformation in prehispanic South Central Andean populations. Int J Osteoarchaeol 23: 459-470. https://doi.org/10.1002/oa.1269
O'Loughlin VD (2004) Effects of different kinds of cranial deformation on the incidence of wormian bones. Am J Phys Anthropol 123: 146-155. https://doi.org/10.1002/ajpa.10304
Okumura M (2014) Differences in types of artificial cranial deformation are related to differences in frequencies of cranial and oral health markers in pre-Columbian skulls from Peru. Boletim do Museu Paraense Emilio Goeldi, Ciencias Humanas 9: 15-26. https://doi.org/10.1590/S1981-81222014000100002
Ossenberg NS (1977) Congruence of distance matrices based on cranial discrete traits, cranial measurements, and linguistic-geographic criteria in five Alaskan populations. Am J Phys Anthropol 47: 93-98.
Pang Z (1993) Artificial cranial deformation, tooth extraction, and ball-holding custom of the prehistoric Dongyi People. Minsu Research: 6.
Pechenkina E, Ma X, Eng J, et al (2009) Reconstructing behaviour in ancient China from human skeletal remains. The SAA Archaeological Record 9: 36-39.
Perez SI (2007) Artificial cranial deformation in South America: a geometric morphometrics approximation. J Archaeol Sci 34: 1649-1658. https://doi.org/10.1016/j.jas.2006.12.003
Profico A, Buzi C, Castiglione S, et al (2021) Arothron: An R package for geometric morphometric methods and virtual anthropology applications. Am J Phys Anthropol 176: 144-151. https://doi.org/10.1002/ajpa.24340
Püschel TA, Friess M, Manríquez G (2020) Morphological consequences of artificial cranial

deformation: Modularity and integration. PloS One15: e0227362. https://doi.org/10.1371/journal.pone.0227362
R Core Team (2025) R: A language and environment for statistical computing. Vienna, Austria: R Foundation for Statistical Computing. Retrieved from https://www.R-project.org/
Rhode MP (2001) Craniofacial morphology and the consequences of intentional cranial deformation among prehistoric Andean populations, University of Nevada, Las Vegas.
Ricci F, Fornai C, Blos VT, et al (2008) Evidence of artificial cranial deformation from the later prehistory of the Acacus Mts. (Southwestern Libya, Central Sahara). Int J Osteoarchaeol 18: 372-391. https://doi.org/10.1002/oa.946
Ross AH, Ubelaker DH (2009) Effect of intentional cranial modification on craniofacial landmarks: a three-dimensional perspective. J Craniofacial Surg 20: 2185-2187. https://doi.org/10.1097/SCS.0b013e3181bf038c
Schijman E (2005) Artificial cranial deformation in newborns in the pre-Columbian Andes. Child's Nervous System 21: 945-950. https://doi.org/10.1007/s00381-004-1127-8
Schlager S (2017) Chapter 9 - Morpho and Rvcg – Shape Analysis in R: R-Packages for geometric morphometrics, shape analysis and surface manipulations. In: Zheng G, Li S, Székely G, Statistical shape and deformation analysis, Academic Press, p. 217-256.
Schweissing M, Grupe G (2000) Local or nonlocal? A research of strontium isotope ratios of teeth and bones on skeletal remains with artificial deformed skulls. Anthropol Anz 58: 99-103. https://doi.org/10.1127/anthranz/58/2000/99
Seguchi N, Loftus JF, III, Yonemoto S, et al (2023) Investigating intentional cranial modification: A hybridized two-dimensional/three-dimensional study of the Hirota site, Tanegashima, Japan. PloS One18: e0289219. 10.1371/journal.pone.0289219
Sikora M, Pitulko VV, Sousa VC, et al (2019) The population history of northeastern Siberia since the Pleistocene. Nature 570: 182-188. https://doi.org/10.1038/s41586-019-1279-z
Solecki R, Akkermans P, Agelarakis A, et al (1992) Artificial cranial deformation in the Proto-Neolithic and Neolithic Near East and its possible origin: Evidence from four sites. Paléorient 18. https://doi.org/10.3406/paleo.1992.4574
Solecki RS, Solecki RL, Agelarakis AP (2004) The proto-neolithic cemetery in Shanidar Cave, Texas A&M University Press.
Suzuki M (1950) Djalainor Skull No. II. J Anthropol Soc Jpn 61: 175-182. https://doi.org/10.1537/ase1911.61.175
Tiesler V (2013) The bioarchaeology of artificial cranial modifications: New approaches to head shaping and its meanings in Pre-Columbian Mesoamerica and beyond, 7, Springer Science & Business Media.
Torres-Rouff C, Yablonsky LT (2005) Cranial vault modification as a cultural artifact: a comparison of the Eurasian steppes and the Andes. Homo 56: 1-16. https://doi.org/10.1016/j.jchb.2004.09.001
Wang X, Tang Z (2020) The first large-scale bioavailable Sr isotope map of China and its implication for provenance studies. Earth-Sci Rev 210: 103353. https://doi.org/10.1016/j.earscirev.2020.103353
Wang X, Tang Z, Wu J, et al (2016) Strontium isotope evidence for a highly mobile population on the Pamir Plateau 2500 years ago. Scientific Reports 6: 35162. https://doi.org/10.1038/srep35162
Waters MR (2019) Late Pleistocene exploration and settlement of the Americas by modern humans. Science 365: eaat5447. https://doi.org/10.1126/science.aat5447
Willerslev E, Meltzer DJ (2021) Peopling of the Americas as inferred from ancient genomics. Nature 594: 356-364. https://doi.org/10.1038/s41586-021-03499-y
Xiao X. (2014) Study of human skeletons from the Houtaomuga Site in Da'an, Jilin, Jilin University.
Yi S, Clark G, Aigner JS, et al (1985) The "Dyuktai Culture" and New World Origins [and Comments and Reply]. Curr Anthropol 26: 1-20.
Yin Q, Li Q, Zhang H, et al (2022) A 10 ka intentionally deformed human skull from Northeast

Asia. Int J Osteoarchaeol 32: 932-937. https://doi.org/10.1002/oa.3104

Zhang L (2010) Study of Human Skeletons from the Jilintai Cemetery in Ili, Xinjiang (Doctoral), Jilin University.

Zhang M, Fu Q (2020) Human evolutionary history in Eastern Eurasia using insights from ancient DNA. Curr Opin Genet Dev 62: 78-84. https://doi.org/10.1016/j.gde.2020.06.009

Zhang Q, Liu P, Yeh H-Y, et al (2019) Intentional cranial modification from the Houtaomuga Site in Jilin, China: Earliest evidence and longest in situ practice during the Neolithic Age. Am J Phys Anthropol 169: 747-756. https://doi.org/10.1002/ajpa.23888

Zhang Z, You Y (1985) A Custom of Prehistoric Chinese Humans: Artificial Cranial Modification. Prehistoric Research 9: 81-86.

Zhao Y, Zeng W, Wei C, et al (2017) Study of Occipital Deformation in the Dawenkou Culture. Southeast Culture: 9.

Associate Editor, Vitale Sparacello